Systems metabolic engineering of *Corynebacterium glutamicum* for efficient L-tryptophan production

Yufei Dong[1], Zhen Chen[1,2]*

[1]Key Laboratory of Industrial Biocatalysis (Ministry of Education), Department of Chemical Engineering, Tsinghua University, Beijing 100084, China

[2]Center for Synthetic and Systems Biology, Tsinghua University, Beijing 100084, China

***Correspondence**

Corresponding author: Zhen Chen

E-mail: zhenchen2013@mail.tsinghua.edu.cn

Tel: +86-10-62772130. Fax: +86-10-62792128

Abstract:

Corynebacterium glutamicum is a versatile industrial microorganism for producing various amino acids. However, there have been no reports of a well-defined *C. glutamicum* strain capable of hyperproducing L-tryptophan. This study presents a comprehensive metabolic engineering approach to establish a robust *C. glutamicum* cell factory for L-tryptophan biosynthesis, including: (1) identification of potential targets using an enzyme-constrained genome-scale model; (2) targeted enhancement of the L-tryptophan biosynthetic pathway; (3) reconfiguration of central metabolic pathways; (4) identification of metabolic bottlenecks through comparative metabolome analysis; (5) engineering of the transport system, shikimate pathway, and precursor supply; and (6) repression of competing pathways and iterative optimization of key targets. The resulting engineered *C. glutamicum* strain achieved a remarkable L-tryptophan titer of 16.2 g/L with a yield of 0.16 g/g glucose in shake-flask fermentation. This study highlights the efficacy of integrating computational modeling with systems metabolic engineering for significantly enhancing the production capabilities of industrial microorganisms.

Key word: L-tryptophan, *Corynebacterium glutamicum*, Metabolic engineering, Transporter engineering, Genome-scale modeling.

1 Introduction

L-tryptophan is an essential amino acid for both animals and human, which plays vital roles in protein synthesis and metabolic regulation. L-tryptophan and its derivatives, such as 5-hydroxy-L-tryptophan (Lee and Lee, 2020; Shen et al., 2020), violacein (Füller et al., 2016; Sarwar et al., 2021), and indigos (Cao et al., 2020; Choi, 2020), are extensively utilized in the pharmaceutical, cosmetic, food, and animal feed industries. Currently, the primary method for L-tryptophan production is microbial fermentation. In particular, metabolic engineering of *Escherichia coli* for the production of L-tryptophan has been intensively studied over the past few years, establishing *E. coli* as the predominant microbial chassis for industrial L-tryptophan production. Much of these research has focused on optimizing the rate-limiting steps in the L-tryptophan synthesis pathway, enhancing the availability of metabolic precursors such as phosphoenolpyruvate (PEP) and erythrose-4-phosphate (E4P), and blocking competing pathways and the L-tryptophan degradation pathway (Chen and Zeng, 2016; Guo et al., 2021; Liu et al., 2023; Wang et al., 2013; Xiong et al., 2021). Furthermore, the development of riboswitch-based biosensors has facilitated the identification of new genetic targets to enhance L-tryptophan production (Tang et al., 2023). By integrating various strategies, engineered *E. coli* strains have achieved L-tryptophan production titers of 40 to 55 g/L and yields of 0.15 to 0.23 g/g glucose in fed-batch fermentation (Guo et al., 2021; Niu et al., 2019; Xiong et al., 2021). However, compared to other amino acids such as L-lysine and L-threonine, the titers and yields of L-tryptophan achieved thus far remain relatively low, substantially below the theoretical yield of L-tryptophan. This discrepancy results in elevated production costs, thereby constraining the broader industrial utilization of L-tryptophan. Accordingly, the development of more robust and efficient microbial strains for L-tryptophan production is highly desirable.

Corynebacterium glutamicum is another important industrial chassis broadly used for the industrial production of amino acids. It offers several advantages over *E. coli* for large-scale amino acid production, including enhanced safety, greater robustness to environmental stress, increased resistance to phage contamination, and the capacity to utilize a wide range of substrates (Chai et al., 2021; Unthan et al., 2014; Zha et al., 2023). Systems metabolic engineering strategies have been employed to engineer *C. glutamicum* microbial cell factories for the high-level production of L-lysine, L-arginine, L-proline, etc (Jiang et al., 2021; Kogure and Inui, 2018; Liu et al., 2022a; Liu et al., 2022b; Zhang et al., 2020; Zhao et al., 2022). Early efforts to establish L-tryptophan production in *C. glutamicum* during the 1990s employed a strategy combining random mutagenesis with a limited number of rational genetic modifications (Ikeda and Katsumata, 1999). This approach resulted in a strain achieving a record L-tryptophan titer of 58 g/L in fed-batch fermentation, highlighting the potential of *C. glutamicum* for high-level production of this amino acid. However, the engineered *C. glutamicum* strain exhibited several limitations, including retarded cell growth and low productivity, potentially attributed to the accumulation of deleterious mutations during repeated rounds of mutagenesis.

Furthermore, the strain's reliance on a large plasmid and the requirement for exogenous L-phenylalanine and L-tyrosine supplementation hindered its suitability for industrial-scale applications. Therefore, the development of a genetically stable and well-defined *C. glutamicum* strain capable of hyperproducing L-tryptophan remains a priority.

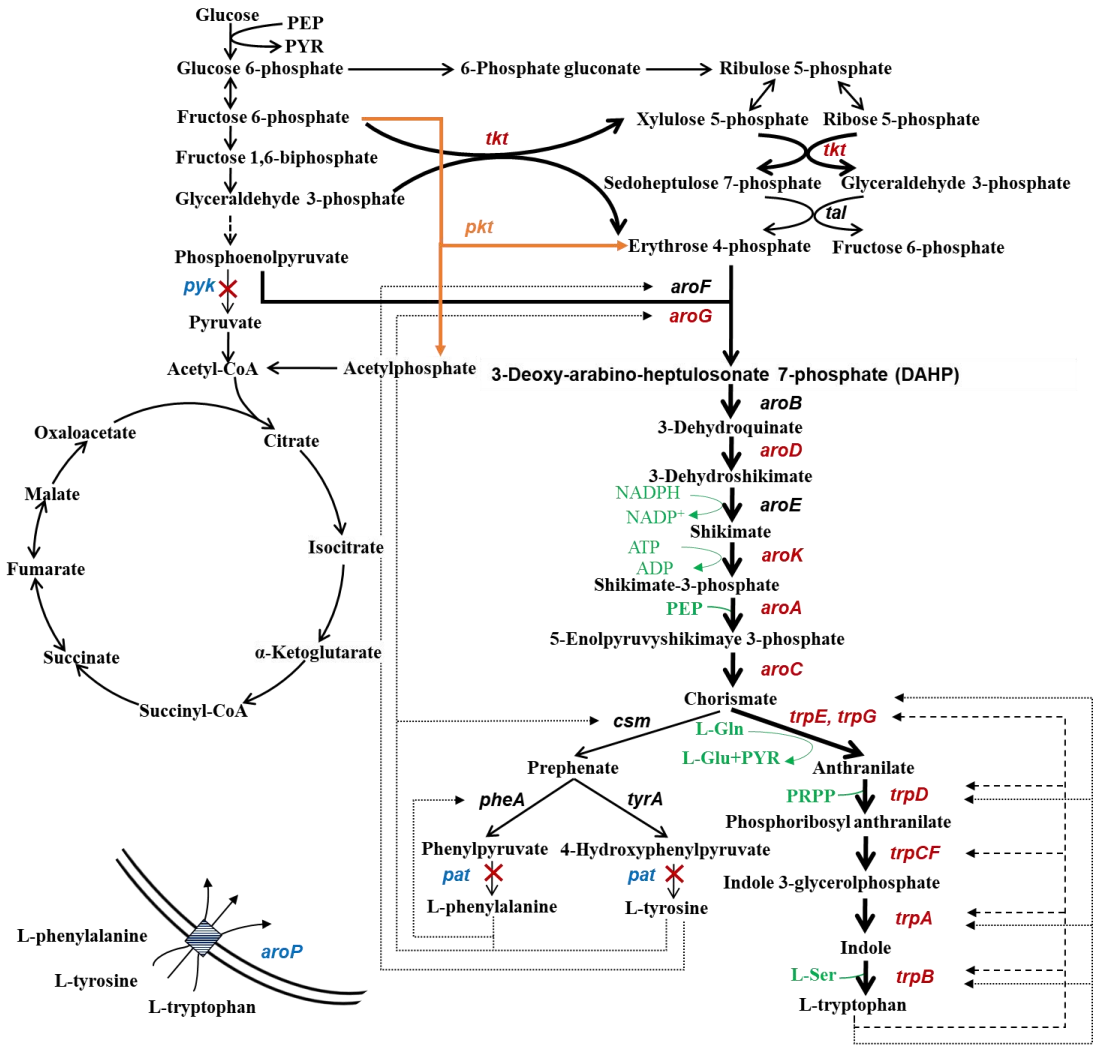

Fig. 1. Systematic metabolic engineering of *C. glutamicum* for L-tryptophan production. The dotted lines and dashed lines indicate feedback inhibition and repression, respectively. Precursors and cofactors are colored in green. The overexpression targets are shown with thick lines and red characters. The deletion or down-regulation targets are shown with thin lines and blue characters. The symbol "X" indicates gene deletion. The introduced exogenous phosphoketolase is colored in orange. PEP, phosphoenolpyruvate; PYR, pyruvate; L-Gln, L-glutamine; L-Ser, L-serine; PRPP, phosphoribosyl diphosphate.

While the rate-limiting steps and metabolic regulation of L-tryptophan biosynthesis in *E. coli* have been extensively studied, these aspects remain largely unexplored in *C. glutamicum*. Additionally, other potential metabolic engineering targets, such as

L-tryptophan exporters or importers, have not been clearly elucidated in *C. glutamicum*. To address this knowledge gap, this study employed the integration of a genome-scale model (GEM) and omics analysis to identify potential metabolic targets. Subsequently, systems metabolic engineering strategies were implemented to engineer a wild-type *C. glutamicum* strain for enhanced L-tryptophan production (Fig. 1). These strategies involved debottlenecking the rate-limiting steps, balancing precursor supply, introducing novel L-tryptophan exporters, and repressing competing pathways. This comprehensive engineering approach enabled the construction of a well-defined *C. glutamicum* strain capable of producing L-tryptophan with a titer of 16.2 g/L and a yield of 0.16 g/g glucose in shake-flask fermentation, without using plasmids or supplementing other essential amino acids. This work lays the foundation for developing an economically viable process for industrial-scale L-tryptophan production.

2 Materials and methods

2.1 Bacterial strains and plasmids

The *C. glutamicum* strains used in this study are listed in Table 1. *E. coli* DH5α was used as the host for plasmid construction. The starting *C. glutamicum* strain MB001 was a prophage-free strain derived from ATCC 13032 (Baumgart et al., 2013). The plasmids used in this study are listed in Table S1. The pK18*mobsacB*-derived plasmids were used for markerless gene deletion and integration in *C. glutamicum*. The pEC-K18*mob2* plasmid (Tauch et al., 2002), an *E. coli* and *C. glutamicum* shuttle vector, was applied for gene overexpression in *C. glutamicum* strains.

2.2 Plasmids and strains construction

Gibson assembly was generally used for plasmid construction following the standard procedures. Gene deletion and insertion in *C. glutamicum* were conducted using the pK18*mobsacB*-derived plasmids through two rounds of recombination (Chen et al., 2017). The codon-optimized phosphoketolase gene from *Bifidobacterium adolescentis* and the aromatic amino acid transporter genes were synthesized by Genewiz Company (Suzhou, China). The aromatic amino acid transporters tested in this study are listed in Table S2.

For the construction of plasmids for gene overexpression, the artificial promoter, the functional gene with a common a RBS (aaaggaggttgtc), and the rrnB terminator were inserted into the restriction sites EcoRI/XbaI of the plasmid pEC-K18*mob2* by Gibson assembly.

Table 1 Strains used in this study

Strains	Charateristics	Source
MB001	Prohage-free variant of *C. glutamicum*	Lab stock
TR01	MB001 with the substitution of promoter of *trp* operon by a strong promoter H36	This work
TR02	TR01, with point mutations in *trpD* (*trpD*$^{S149F/A162E}$)	This work
TR03	TR02 with genome integration of *aroG*^{D146N} from *E. coli* and *serA*$^{\Delta 197}$ from *C. glutamicum* under the control of *tuf* promoter	This work
TR04	TR03 with genome integration of *trpE*^{S40F}-*trpD* from *E. coli* under the control of *tuf* promoter at the intergenetic region between *cgp_1121* and *cgp_1122*	This work
TR05	TR04 with genome integration of *trpCBA* from *E. coli*	This work
TR06	TR05 with replacement of genome-integrated *trpD* from *E. coli* by *trp4* from *Saccharomyces cerevisiae*	This work
TR07	TR06 with deletion of *pyk*	This work
TR08	TR07 with insertion of a H36 promoter before *tkt* and change of *tkt* start codon from ttg to atg	This work
TR09	TR07 with genome integration of phosphoketolase gene mutant *pkt*$^{T2A/I6T/H260Y}$ from *Bifidobacterium adolescentis* under the control of *tuf* promoter into *bioA*	This work
TR10	TR07 with genome integration of phosphoketolase gene mutant *pkt*$^{T2A/I6T/H260Y}$ from *B. adolescentis* under the control of H36 promoter into *bioA*	This work
TR11	TR07 with genome integration of phosphoketolase gene from *B. adolescentis* under the control of *tuf* promoter into *bioA*	This work
TR12	TR07 with genome integration of phosphoketolase gene from *B. adolescentis* under the control of H36 promoter into *bioA*	This work
TR13	TR09 with deletion of *ldh*	This work
TR14	TR13 with genome integration of *yddG* from *Herbaspirillum rhizosphaerae* under the control of H36 promoter into *crtB2*	This work
TR15	TR13 with genome integration of *yddG* from *Paraburkholderia acidisoli* under the control of H36 promoter into *crtB2*	This work
TR16	TR13 with genome integration of *yddG* from *Herbaspirillum aquaticum* under the control of H36 promoter into *crtB2*	This work
TR17	TR13 with genome integration of *yddG* from *H. rhizosphaerae* under the control of *tuf* promoter into *crtB2*	This work
TR18	TR13 with genome integration of *yddG* from *P. acidisoli* under the control of *tuf* promoter into *crtB2*	This work
TR19	TR13 with genome integration of *yddG* from *H. aquaticum* under the control of *tuf* promoter into *crtB2*	This work
TR20	TR14 with genome intergration of *aroDC* from *C. glutamicum* under the control of H36 promoter into *crtI2*	This work

TR21	TR14 with genome intergration of *aroDC* from *C. glutamicum* under the control of *tuf* promoter into *crtI2*	This work
TR22	TR21 with genome integration of *glnA*^{E304A} from *Bacillus subtilis* and *prsA* from *C. glutamicum* MB001 under the control of H36 promoter into *crtYf*	This work
TR23	TR22 with genome integration of *tkt* from *C. glutamicum* under the control of H36 promoter into *bioD*	This work
TR24	TR23 with deletion of *pat*	This work
TR25	TR24 with deletion of *aroP*	This work
TR26	TR24 with genome integration of *aroG*^{D146N} from *E. coli* under the control of H36 promoter behind the genome-integrated *tkt* at the *bioD* locus	This work

2.3 Genome-scale metabolic modeling

To calculate the optimal metabolic flux distribution for biomass or L-tryptophan biosynthesis, flux balance analysis (FBA) was conducted based on the genome-scale enzyme-constrained model (ecCGL1) (Niu et al., 2022) of *C. glutamicum* using the CAVE platform (Mao et al., 2023). The D-glucose uptake rate was set as 100, and the oxygen uptake rate was set as 1000 for aerobic condition. The objective product was selected as biomass or L-tryptophan.

To predict the specific metabolic engineering targets for L-tryptophan production, protein costs disparities between high growth low product generation (HGLP) (growth rate set as 0.46 h^{-1}) and low growth high product generation (LGHP) (growth rate set as 0.1 h^{-1}) situations were calculated based on ecCGL1 using ECMpy 2.0 (Mao et al., 2024). The glucose uptake rate was set as 10 mmol·gDW^{-1} h^{-1}. Reactions with fold changes in enzyme costs over 1.5 between LGHP and HGLP conditions were selected as metabolic engineering targets (Niu et al., 2022). The calculation was conducted in Python 3.12, and the code was obtained from the previous research (Mao et al., 2024).

2.4 Medium and culture conditions

For shake-flask fermentations, *C. glutamicum* strains were first cultured in 20 mL LSS1 medium in 250 mL baffled shake flasks at 30 °C, 200 rpm for 14-16 h (Wu et al., 2019). The seed cultures were subsequently inoculated into 30 mL LPG2 medium in 500 mL baffled shake flasks with 30 g/L of $CaCO_3$ (Li et al., 2022) to perform L-tryptophan fermentations. The initial concentration of glucose was 100 g/L. All shake-flask fermentations were conducted in duplicate at 30 °C, 200 rpm and an initial pH of 7.2. When necessary, 25 μg/L kanamycin was added.

150 **2.5 Analysis of cell growth and extracellular metabolites**

151 Cell growth was detected by measuring the optical density of 600 nm (OD_{600}) of the
152 samples. The concentrations of glucose, lactic acid, and acetic acid were
153 quantitatively analyzed by high-performance liquid chromatography (HPLC)
154 equipped with an Aminex HPX-87H Column (300×7.8 mm) using 5 mM H_2SO_4 as
155 the mobile phase. The flow rate was set as of 0.8 mL/min at 65 ℃ and the injection
156 volume was 20 μL.

157 The concentrations of L-tryptophan were determined by HPLC with a Dikma
158 Diamonsil AAA Column (5μm, 250×4.6 mm) using the standard phenyl
159 isothiocyanate derivative method (Cohen and Strydom, 1988). L-tryptophan was
160 separated by using mobile phase A (50 mM CH_3COONa, pH 6.5) and phase B
161 (methanol: acetonitrile: water=1: 3: 1) with gradient elution at a total flow rate of 1
162 mL/min at 45 ℃. The detective wavelength was 254 nm and the injection volume was
163 10 μL.

164 **2.6 Metabolome analysis**

165 Intracellular metabolites in *C. glutamicum* cells were extracted as follows. Cells were
166 cultured to the exponential phase and 2 mL of each sample were taken. The cell
167 suspension was centrifuged at 4 ℃, 12000 rpm for 1 min to remove the medium. The
168 cell pellets were washed gently with PBS buffer (pH=7.2-7.4) three times and the
169 supernatant was removed. Afterwards, 1.6 mL of pre-cooled (-80 ℃) 80% methanol
170 was added immediately to resuspend the cell pellets by vortex. The samples were then
171 incubated at -20 ℃ for 30 min and processed by ultra-sonication for 2 min, followed
172 by incubation at -80 ℃ for 2 h for cell lysis. The suspension was subsequently
173 centrifuged at 4 ℃, 14000 rpm for 15 min to remove the protein. The supernatant was
174 taken into a new 2 mL microcentrifuge tube, dried by vacuum and stored at -80 ℃ for
175 further operation.

176 The metabolites in the supernatant were analyzed by using SCIEXTriple Quad 6500+
177 liquid chromatography-tandem mass spectrometry (LC-MS/MS) system (AB Sciex,
178 Singapore) equipped with IonDrive detector and Qtrap-6500 mass spectrometer.

179 **3 Results and discussion**

180 **3.1 Identification of potential engineering targets by genome-scale metabolic**
181 **modeling**

182 As mentioned before, the metabolic regulation and rate-limiting reactions for

L-tryptophan biosynthesis in *C. glutamicum* have not been comprehensively elucidated. Genome-scale metabolic modeling is a powerful tool for predicting cellular phenotypes and serves as an invaluable approach for guiding metabolic engineering strategies to enhance chemical production (Fang et al., 2020). Recently, the first enzyme-constrained model for *C. glutamicum*, ecCGL1, has been developed (Niu et al., 2022). This model incorporates enzyme kinetic data and outperforms the widely used stoichiometry-based model iCW773 in predicting phenotypes and identifying engineering targets (Niu et al., 2022). Therefore, we employed ecCGL1 to predict potential engineering targets for L-tryptophan production.

First, the theoretical yield of L-tryptophan and the optimized metabolic flux distribution was calculated based on the stoichiometric data of ecCGL1 using the CAVE platform (Mao et al., 2023). As illustrated in Fig. 2A, the theoretical yield of L-tryptophan in *C. glutamicum* is 0.435 mol/mol glucose, which is slightly higher than that in *E. coli* (0.414 mol/mol glucose) (Varma et al., 1993). To achieve the theoretical maximum yield of L-tryptophan, the metabolic fluxes toward transketolase reaction involved in E4P biosynthesis, the shikimate pathway, and the terminal steps of L-tryptophan biosynthesis pathway must be significantly enhanced compared to those optimized for cell growth (Fig. 2A). Moreover, the fluxes toward the biosynthesis of key metabolic precursors, including L-serine, L-glutamine, and phosphoribosyl diphosphate (PRPP), should also be increased (Fig. 2A). Conversely, the fluxes involved in the conversion of PEP to pyruvate via the phosphotransferase system (PTS), PEP carboxylase, and pyruvate kinase, as well as flux into tricarboxylic acid (TCA) cycle, must be significantly reduced (Fig. 2A). These predicted results are generally consistent with those previously implemented in *E. coli* (Chen and Zeng, 2016; Guo et al., 2021; Liu et al., 2023; Wang et al., 2013; Xiong et al., 2021), suggesting that the genome-scale metabolic modeling is reliable.

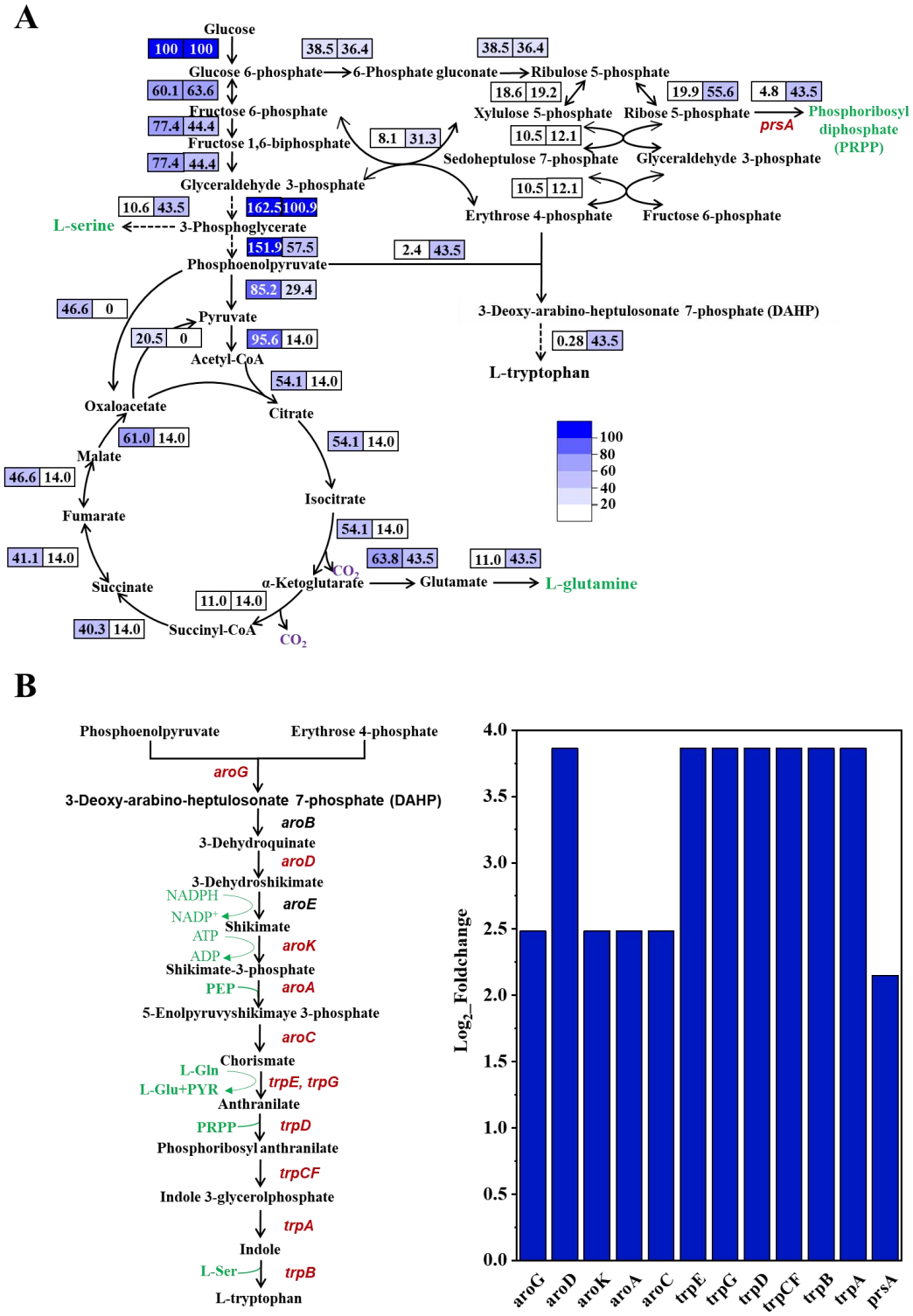

Fig. 2 Metabolic engineering targets prediction for L-tryptophan production by using the ecCGL1 model. (A) Metabolic flux distribution with the objective set as biomass accumulation (numbers on the left) and L-tryptophan production (numbers on the right). (B) Enhanced genetic targets identified by the approach of HGLP/LGHP. Precursors and cofactors are colored in green. The predicted targets are colored in red.

While classical FBA based on stoichiometric balance could provide insights into

potential up- and down-regulated metabolic pathways, it cannot be used to identify key targets within linear pathways. To overcome this limitation, we employed the ecCGL1 model with the constraints of enzyme kinetic data to pinpoint crucial enzymes based on protein cost discrepancies between HGLP and LGHP conditions (Mao et al., 2024). This analysis revealed twelve potential targets with >1.5-fold changes in enzyme cost between HGLP and LGHP states (Fig. 2B and Table S3). These targets could be functionally categorized into three modules: (1) genes (*trpE, trpG*, *trpD*, *trpCF*, *trpB,* and *trpA*) encoding key enzymes within the terminal L-tryptophan biosynthesis pathway, consistent with their roles in L-tryptophan overproduction (Ikeda and Katsumata, 2014; Niu et al., 2019); (2) shikimate pathway genes (*aroG*, *aroD*, *aroK, aroA*, *aroC*), similarly reported to be important for L-tryptophan synthesis in *E. coli* (Liu et al., 2023); (3) *prsA* gene encoding ribose-phosphate diphosphokinase, responsible for catalyzing the synthesis of L-tryptophan precursor PRPP. This study further elucidated the specific roles of these genes in modulating L-tryptophan production in *C. glutamicum*.

3.2 Enhancement of L-tryptophan synthesis pathway

Genome-scale metabolic modeling indicated that enhanced expression of enzymes within the shikimate and L-tryptophan biosynthetic pathways is crucial for increased L-tryptophan production (Fig. 2B). To enhance the L-tryptophan synthesis pathway, we initially attempted to increase the expression of the entire *trp* operon in *C. glutamicum*. In *E. coli*, the *trp* operon is subject to both feedback repression by the TrpR repressor and transcriptional attenuation mediated by the *trpL* leader sequence (Fig. 3A). While *C. glutamicum* also utilizes *trpL*-mediated attenuation (Fig. 3A), a TrpR homologue is absent in its genome. Therefore, to deregulate the *trp* operon in *C. glutamicum* MB001, the native promoter was replaced with the strong constitutive promoter H36, generating strain TR01. Shake-flask fermentation of TR01 yielded only 0.15 g/L L-tryptophan, demonstrating that increased expression of *trpEGDCFBA* alone is insufficient for substantial overproduction (Fig. 3B). Enzyme-constrained metabolic modeling revealed that anthranilate phosphoribosyl transferase (TrpD) is required with high demand for L-tryptophan biosynthesis (Fig. 2B). Furthermore, unlike its *E. coli* homologue, *C. glutamicum* TrpD is subject to feedback inhibition by L-tryptophan (Fig. 1). To alleviate this inhibition, point mutations S149F/A162E were introduced into TrpD of strain TR01 (O'Gara and Dunican, 1995), creating strain TR02. This modification significantly increased L-tryptophan production to 2.70 g/L (Fig. 3B), establishing TrpD as a key control point in *C. glutamicum* L-tryptophan biosynthesis. This contrasts with *E. coli*, where the relief of feedback inhibition by L-tryptophan of anthranilate synthase subunit TrpE rather than TrpD is significant for L-tryptophan production (Caligiuri and Bauerle, 1991)

In addition to TrpD, the 3-deoxy-D-arabino-heptulosonate 7-phosphate (DAHP) synthase, which catalyzes the condensation of PEP and E4P to DAHP, is another

critical enzyme controlling metabolic flux towards aromatic amino acid biosynthesis (Fig. 2B). Given the feedback inhibition of the native DAHP synthases (AroG and AroF) by aromatic amino acids (Ikeda, 2006), a feedback-resistant DAHP synthase variant, AroG^{D146N} from *E. coli* (Kikuchi et al., 1997), was genomically integrated into strain TR02 under the control of tuf promoter. Furthermore, to enhance the biosynthesis of the L-tryptophan precursor L-serine, a copy of feedback-resistant D-3-phosphoglycerate dehydrogenase gene *serA*$^{\Delta 197}$ from *C. glutamicum* (Peters-Wendisch et al., 2002) was also integrated after the heterogeneous *aroG*^{D146N} gene. The resulting strain TR03 exhibited an improved L-tryptophan production of 3.37 g/L (Fig. 3B), suggesting that augmenting the supply of precursors via the expression of feedback-resistant *aroG* and *serA* effectively promotes L-tryptophan overproduction (Ikeda and Katsumata, 1999; Ikeda et al., 2014).

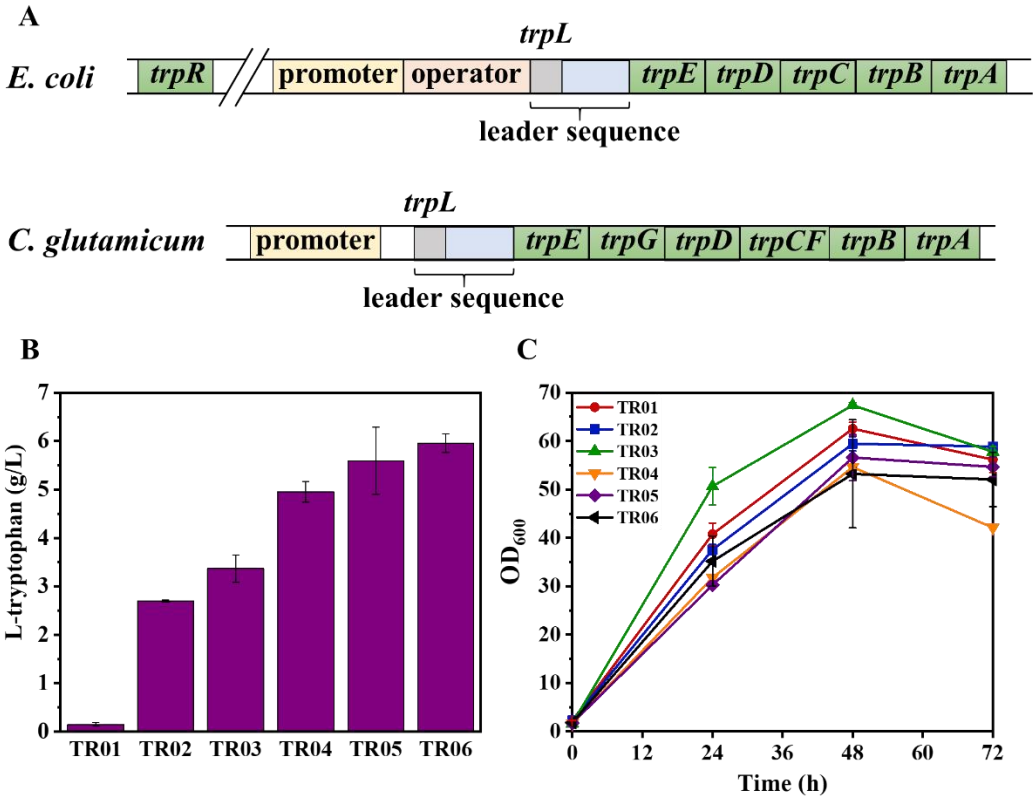

Fig. 3. Engineering of L-tryptophan biosynthesis pathway. (A) The *trp* operon in *E. coli* and *C. glutamicum*. (B) L-tryptophan production. (C) Cell growth.

To further enhance L-tryptophan production, we sought to optimize the L-tryptophan biosynthesis pathway as informed by enzyme-constrained metabolic modeling (Fig. 2B). Specifically, the *trpE*^{S40F}-*trpD* and *trpC-trpB-trpA* gene clusters from *E. coli* were sequentially integrated into the genome of TR03 under the control of the *tuf* promoter, resulting in the generation of strains TR04 and TR05, respectively. The *trpE*^{S40F} encodes a feedback-resistant anthranilate synthase. The L-tryptophan production by both TR04 and TR05 was elevated, with strain TR05 achieving a titer of 5.60 g/L (Fig. 3B). Furthermore, given that TrpD was predicted to be a critical

target within the L-tryptophan biosynthesis pathway (Fig. 2B), we sought to enhance its activity by incorporating a more efficient variant. Previous studies have reported that the TrpD from *Saccharomyces cerevisiae* encoded by *trp4* gene displays a higher affinity for PRPP and greater enzymatic activity compared to the TrpD from *E. coli* (Jun et al., 2015). Consequently, we substituted the *E. coli*-derived *trpD* in TR05 with *trp4* from *S. cerevisiae*, yielding strain TR06. This modification resulted in a further increase in L-tryptophan production to 5.96 g/L (Fig. 3B), confirming its significant role for affecting L-tryptophan overproduction.

3.3 Enhancement of PEP and E4P supply

After optimizing the terminal L-tryptophan biosynthesis pathway, efforts were directed towards enhancing the supply of PEP and E4P, the two direct precursors of aromatic amino acids. To increase PEP availability, the *pyk* gene in strain TR06 was deleted, thereby blocking the conversion of PEP to pyruvate via pyruvate kinase. The resulting strain TR07 exhibited a 22.0% increase in L-tryptophan titer (Fig. 4A). Additionally, an increase in both glucose consumption rate (Fig. S1) and L-tryptophan synthesis rate (Fig. 4A) was observed, suggesting that elevating PEP supply positively impacts glucose consumption through the PTS and L-tryptophan biosynthesis via DAHP synthase.

To further augment E4P supply, two distinct strategies were employed. Initially, we endeavored to boost transketolase activity in strain TR07 by inserting a strong H36 promoter upstream of the endogenous *tkt* gene and substituting its start codon from ttg to atg. However, this modification did not yield an improvement in L-tryptophan yield in the resulting strain TR08 (Fig. 4A). Consequently, an alternative E4P synthesis pathway was explored by introducing a heterologous phosphoketolase. Previous studies have demonstrated that the phosphoketolase from *Bifidobacterium adolescentis* could efficiently convert fructose 6-phosphate (F6P) to E4P and acetylphosphate (Wang et al., 2021), and this enzyme has been successfully applied to enhance aromatic amino acid production (Xiong et al., 2021). Consequently, both the wild-type *pkt* gene and its mutant variant $pkt^{T2A/I6T/H260Y}$, which encodes an enzyme with higher specific activity (Dele-Osibanjo et al., 2019), were introduced into strain TR07 under the control of either the *tuf* or H36 promoters, generating strains TR09-TR12 (Fig. 4C). These strains exhibited varied responses in terms of cell growth, L-tryptophan production, and lactate accumulation (Fig. 4). Notably, strain TR09 demonstrated the most significant improvement in L-tryptophan titer, showing a 10.6% increase over the control strain TR07 (Fig. 4C). Furthermore, cell growth in TR09 was comparable to that of TR07 (Fig. 4D), while lactate accumulation was notably reduced (Fig. 4E). These findings underscored the importance of optimizing *pkt* expression and phosphoketolase activity to balance cell growth with L-tryptophan production. Given the observed lactate accumulation during L-tryptophan production, the *ldh* gene encoding lactate dehydrogenase was deleted in strain TR09. The resulting strain TR13 exhibited a 12.8% increase in L-tryptophan

321 titer compared to TR09, with no detectable lactate accumulation during fermentation
322 (Fig. 4).

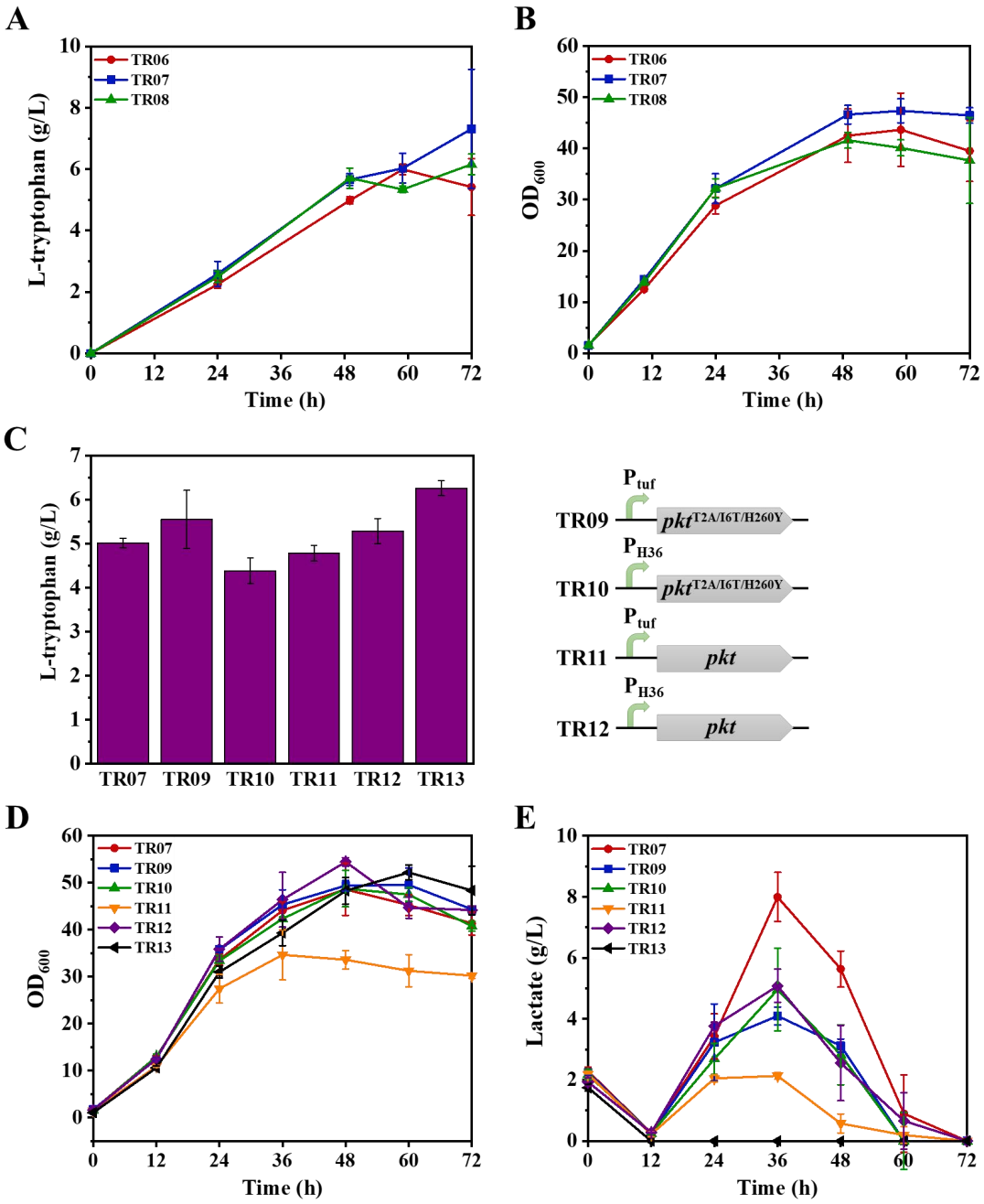

323

324 **Fig. 4. Engineering of the central metabolic pathways.** (A) L-tryptophan
325 production by strains TR07 and TR08. (B) Cell growth. (C) L-tryptophan production.
326 (D) Cell growth. (E) Lactate accumulation.

327 **3.4 Metabolome analysis**

328 To elucidate alterations in cellular metabolism and potential bottlenecks hindering

L-tryptophan production, a comparative metabolome analysis was conducted between the engineered strain TR09 and the wild-type strain MB001. This analysis focused on central metabolic pathway intermediates and intracellular amino acids. As illustrated in Fig. 5A, a total of 110 metabolites within central metabolic pathways were quantified, with significant increases observed in 32 metabolites and significant decreases in 27 metabolites within the TR09 strain (Table S4). Notably, most metabolites in the glycolysis pathway exhibited elevated concentrations in TR09, except for F6P. This exception is possibly due to the introduction of phosphoketolase, which results in the conversion of F6P to E4P. Moreover, the concentrations of PEP and most metabolites in the pentose phosphate pathway were elevated, indicating no apparent supply limitation of PEP and E4P (Fig. S2). Importantly, the concentration of shikimate in TR09 increased by 298-fold, indicating that optimizing the downstream portion of the shikimate pathway to reduce shikimate accumulation is essential for improving L-tryptophan production.

Regarding the change in intracellular amino acids, TR09 showed significant increases in 4 amino acids and decreases in 9 amino acids compared to MB001 (Fig. 5B and Table S4). In particular, the intracellular levels of L-tryptophan and L-tyrosine in TR09 were elevated by 787-fold and 22.5-fold, respectively. This suggests that enhancing L-tryptophan export and reducing L-tyrosine biosynthesis could be potential strategies for increasing L-tryptophan production. Conversely, a pronounced decrease in the concentrations of L-glutamine and PRPP was observed in TR09, indicating that increasing the availability of these two precursors may be necessary to boost L-tryptophan production. Overall, this metabolome analysis provided new targets for further enhancing L-tryptophan production.

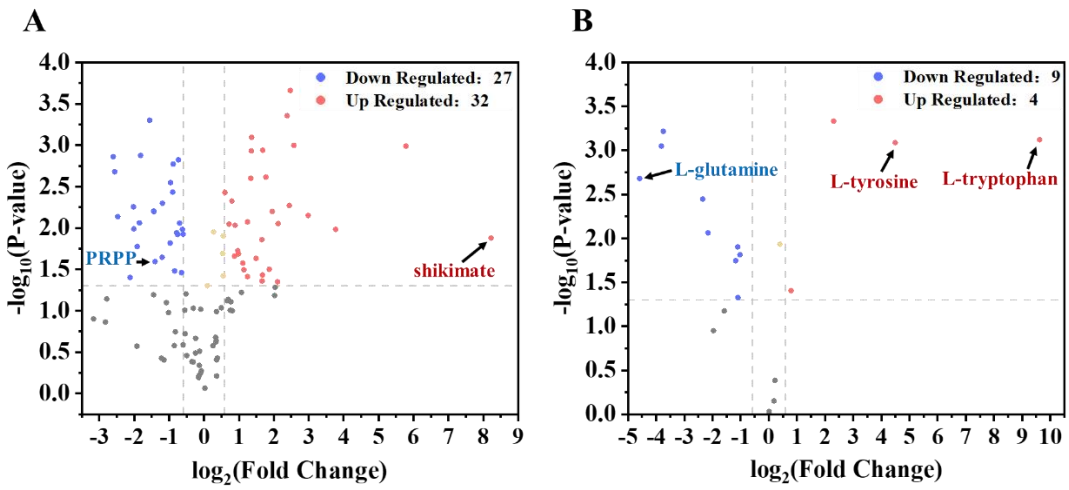

Fig. 5. Comparative metabolome analysis of TR09 and MB001. (A) Volcano plot depicting changes of intracellular metabolites within central metabolic pathways. (B) Volcano plot depicting changes of intracellular amino acids. Metabolites with average fold change ≥1.5, t-test p ≤0.05 were considered significantly different.

358 **3.5 Transporter engineering to increase L-tryptophan production**

359 The metabolome analysis revealed a substantial accumulation of intracellular
360 L-tryptophan in strain TR09. Consequently, enhancing the export of L-tryptophan
361 could mitigate its cellular toxicity and alleviate the feedback inhibition imposed on
362 enzymes in the L-tryptophan biosynthesis pathway. Given that no endogenous
363 L-tryptophan exporter has been identified in *C. glutamicum*, we employed
364 PSI-BLAST to identify potential L-tryptophan exporters in the Uniprot database,
365 using the sequence of the *E. coli* L-tryptophan exporter YddG as a query (Tang et al.,
366 2023). Seven candidate exporters were selected (Table S2), and the corresponding
367 genes were subsequently overexpressed in strain TR13 with plasmid pEC-K18*mob2*
368 (Fig. 6A). Strains overexpressing *yddG* from *Herbaspirillum rhizosphaerae* (Hrh),
369 *Herbaspirillum aquaticum* (Haq), and *Paraburkholderia acidisoli* (Pac) exhibited the
370 most significant increase in L-tryptophan titers (Fig. 6A). Subsequently, the three
371 selected *yddG* genes were individually integrated into the genome of strain TR13
372 under the control of either the H36 or *tuf* promoter, resulting in the generation of
373 strains TR14 to TR19 (Fig. 6C). All engineered strains demonstrated a
374 substantial increase in L-tryptophan titer (Fig. 6C) without compromising cellular
375 growth (Fig. 6B). Specifically, strain TR14, harboring the integrated *H. rhizosphaerae*
376 *yddG* gene under the H36 promoter, achieved the highest L-tryptophan titer of 11.24
377 g/L, which is 2.1-folds higher than that of strain TR13 (Fig. 6C). These findings
378 suggest that L-tryptophan export represents a critical bottleneck in L-tryptophan
379 production in *C. glutamicum*. Therefore, screening for and optimizing the expression
380 of appropriate *yddG* genes is essential for enhancing L-tryptophan production in this
381 organism.

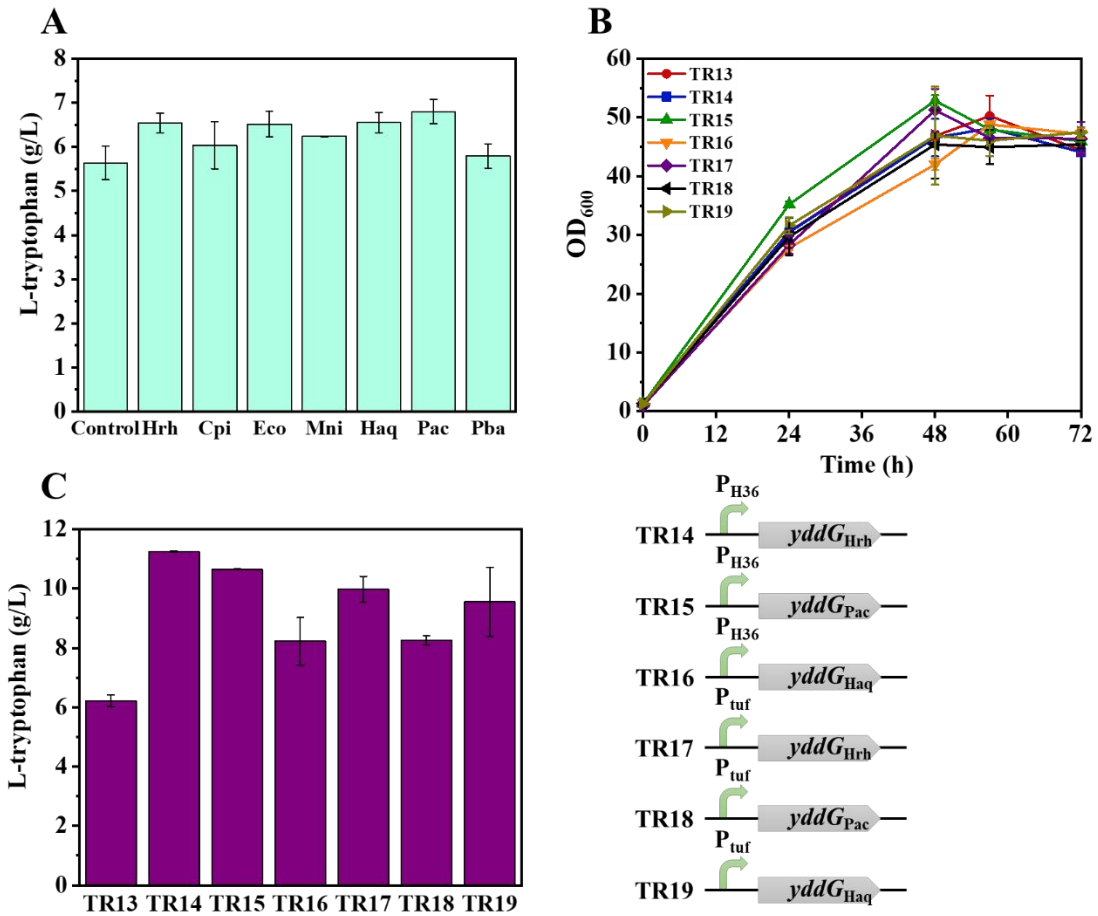

Fig. 6. Screening of L-tryptophan exporters. (A) Screening of potential L-tryptophan exporters with plasmid pEC-K18*mob2*. The control group contained an empty pEC-K18*mob2* plasmid. (B) Cell growth of the engineered strains. (C) L-tryptophan production by strains with integrated L-tryptophan exporters in genome.

3.6 Optimization of the shikimate pathway

Given the significant accumulation of shikimate observed in the metabolome analysis of strain TR09 (Fig. 5), it is necessary to optimize the shikimate pathway to redirect metabolic flux toward L-tryptophan production. Enzyme-constrained metabolic modeling indicated that the genes *aroD*, *aroK*, *aroA*, and *aroC* are potential targets within the shikimate pathway (Fig. 2B). To investigate this prediction, each of these genes was individually overexpressed in strain TR09 with plasmid pEC-K18*mob2*. Overexpression of *aroA* did not significantly impact L-tryptophan production, while *aroK* overexpression resulted in a decrease in L-tryptophan titer (Fig. 7A). Conversely, overexpression of either *aroC* or *aroD* led to a 15.8% increase in L-tryptophan titer (Fig. 7A), suggesting that the native expression levels of these genes may limit L-tryptophan biosynthesis in *C. glutamicum*. To further validate the general applicability of these findings, the *aroD* and *aroC* genes were simultaneously integrated into the genome of strain TR14 under the control of either the H36 or tuf

promoter, resulting in the creation of strains TR20 and TR21, respectively. Both TR20 and TR21 demonstrated enhanced L-tryptophan production, with strain TR21 achieving the highest titer, a 20.1% improvement compared to the parental strain TR14 (Fig. 7B). Additionally, cell growth of TR20 and TR21 was not negatively affected (Fig. 7C).

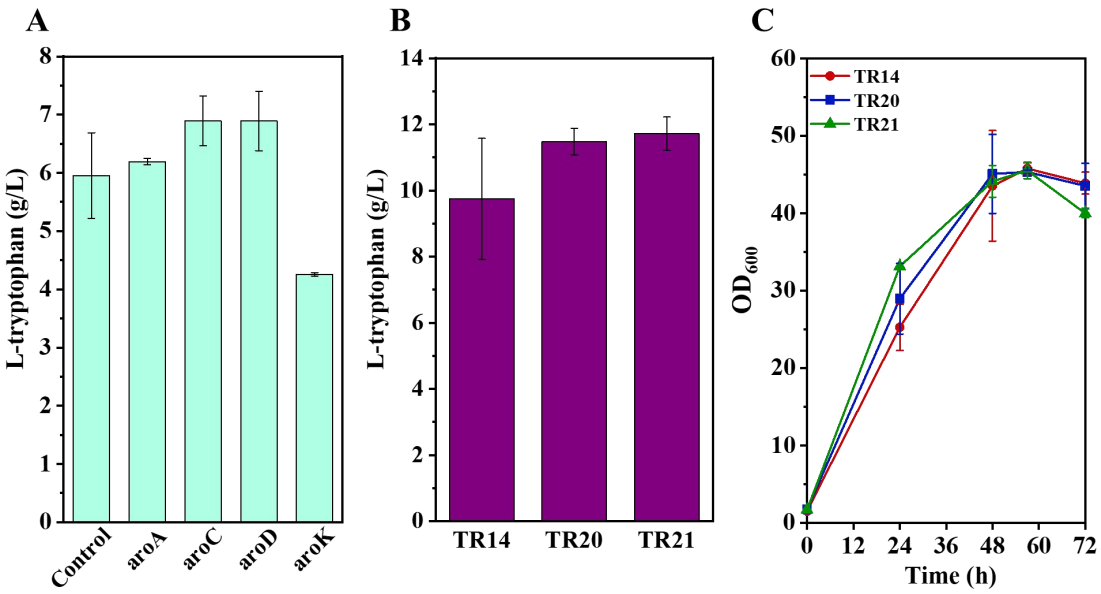

Fig. 7. Optimization of the shikimate pathway. (A) L-tryptophan production by strains overexpressing *aroA*, *aroC*, *aroD*, and *aroK* genes. (B) L-tryptophan production by simultaneously overexpressing *aroD-aroC* genes. (C) Cell growth of the engineered strains.

3.7 Optimization of the availability of other precursors

Metabolome analysis revealed significantly reduced intracellular concentrations of L-glutamine and PRPP in TR09 (Fig. 5), suggesting that increasing the availability of these precursors may enhance L-tryptophan production. To increase the supply of L-glutamine and PRPP, four *glnA* genes encoding glutamine synthetases and three *prsA* genes encoding PRPP synthetase from various organisms (Table S5), which were characterized with high enzymatic activities (Lv et al., 2021), were individually overexpressed in strain TR14 with plasmid pEC-K18*mob2* (Lv et al., 2021). All strains overexpressing *glnA* exhibited increased L-tryptophan production while those overexpressing *prsA* from *E. coli* or *C. glutamicum* also demonstrated elevated L-tryptophan titers (Fig. 8A). The most significant improvements were observed in strains overexpressing the feedback-resistant $glnA^{E304A}$ from *Bacillus subtilis* (Wray and Fisher, 2010) and the native *prsA* from *C. glutamicum* (Fig. 8A). Consequently, the $glnA^{E304A}$ gene from *B. subtilis* and the *prsA* gene from *C. glutamicum* were co-integrated into the genome of TR21, creating strain TR22. The L-tryptophan production by strain TR22 was increased to 12.0 g/L, representing a 6.6%

enhancement in L-tryptophan yield compared to strain TR21 (Fig. 8B). Moreover, the cell growth of TR22 was also improved (Fig. 8C).

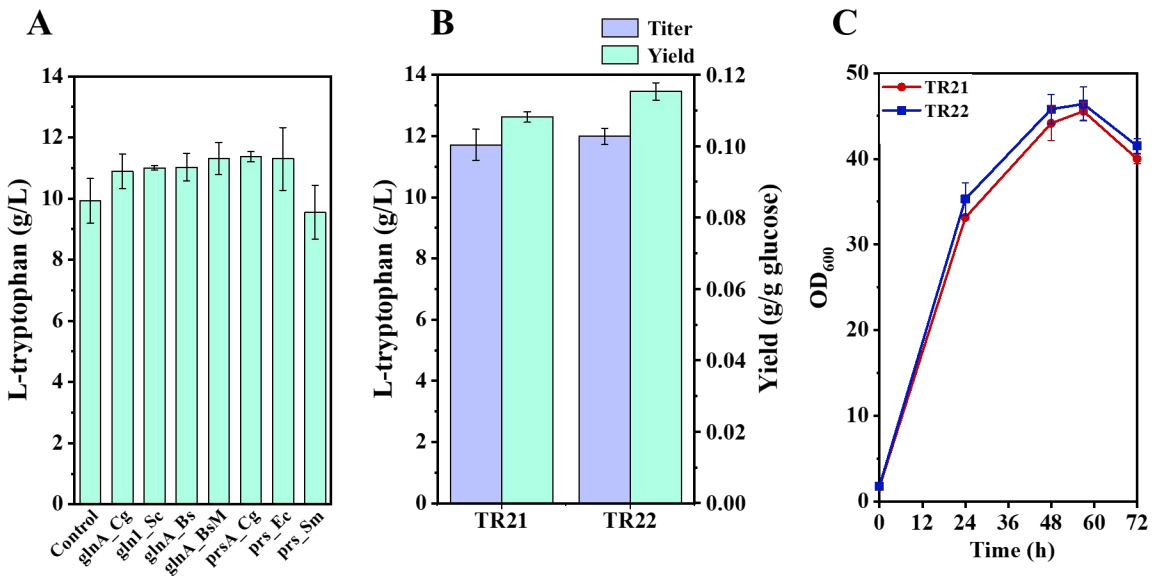

Fig. 8. Increasing of the supply of glutamine and PRPP to enhance L-tryptophan production. (A) L-tryptophan production by strains overexpressing glutamine synthetase and PRPP synthetase genes. (B) L-tryptophan production by simultaneously overexpressing *glnA*_BsM-*prsA*_Cg genes. (C) Cell growth of the engineered strains.

3.8 Iterative optimization of key targets and knockdown of competing pathways

Although the production of L-tryptophan by strain TR22 was significantly enhanced through the integration of various metabolic engineering strategies, the resulting titer remains insufficient for industrial application. Recognizing that new bottlenecks may emerge during the engineering process, an iterative optimization approach was employed to fine-tune the supply of precursors and the L-tryptophan biosynthesis pathway. First, to ensure an adequate supply of E4P, an additional copy of the *tkt* gene under the control of the H36 promoter was integrated into the genome of TR22, generating strain TR23. The production of L-tryptophan by strain TR23 increased to 13.7 g/L (Fig. 9A), indicating that E4P shortage had emerged during the construction of strain TR22.

Subsequently, to reduce the metabolic flux toward the biosynthesis of other aromatic amino acids, the *pat* gene encoding prephenate aminotransferase was deleted in TR23. The resulting strain TR24 exhibited a further increase in L-tryptophan titer to 15.4 g/L (Fig. 9A). Notably, the cell growth of strain TR24 was unaffected, suggesting that other non-specific aminotransferases can compensate for the synthesis of L-pheneyalanine and L-tyrosine (Fig. 9B). To block L-tryptophan uptake, the aromatic amino acid importer gene *aroP* (Shang et al., 2013) was deleted in strain

TR24, generating strain TR25. However, this modification resulted in a slight reduction in L-tryptophan titer (Fig. 9A) as well as decreased glucose consumption rate (Fig. 9C), indicating the import of L-tryptophan is not a limiting factor for L-tryptophan production in *C. glutamicum*.

In an effort to further increase flux through the shikimate pathway, an additional copy of *aroG*^{D146N} from *E. coli* was integrated into the genome of strain TR24. The resulting strain TR26 showed an improved L-tryptophan titer of 16.2 g/L (Fig. 9A) with a yield of 0.16 g/g glucose, which is comparable to the reported yield in *E. coli*. These findings underscore the necessity of iterative optimization in strain engineering to address emerging bottlenecks and achieve higher product titers.

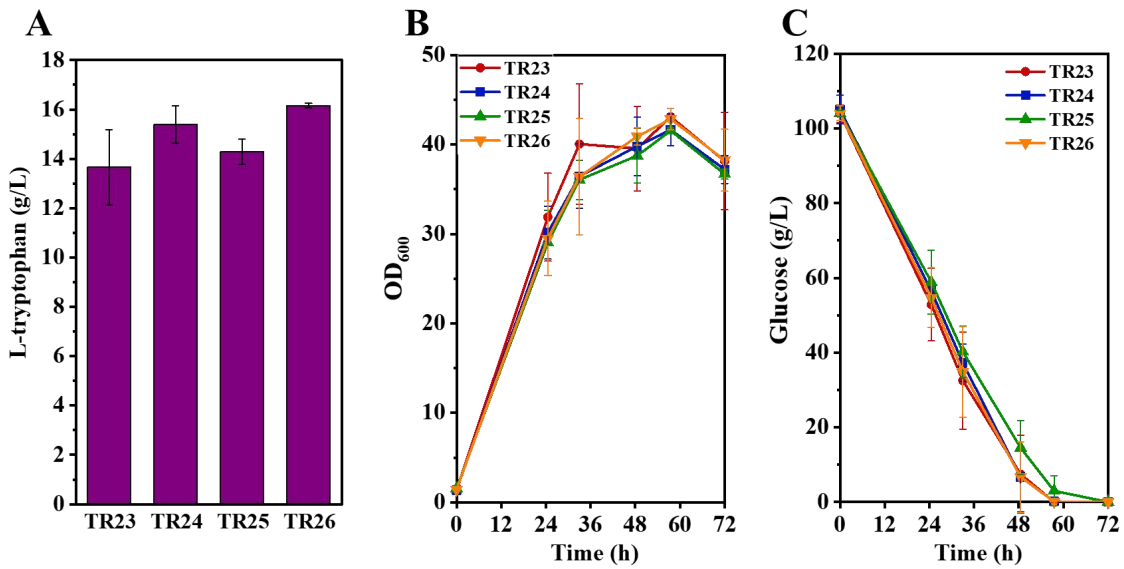

Fig. 9. Iterative optimization of the L-tryptophan-producing strain. (A) L-tryptophan production of the engineered strains. (B) Cell growth of the engineered strains. (C) Glucose uptake of the engineered strains.

4 Conclusion

In conclusion, this study successfully engineered L-tryptophan-overproducing *C. glutamicum* strains with a defined genetic background using a systems metabolic engineering approach. By integrating enzyme-constrained genome-scale metabolic modeling (ecCGL1) and comparative metabolome analysis, a series of key targets for enhancing L-tryptophan biosynthesis, including *trpD*, *aroC*, *aroD*, and others, were identified, highlighting differences in metabolic regulation compared to *E. coli*. Furthermore, the overexpression of heterologous phosphoketolase, glutamine synthetases, and PRPP synthetase, coupled with the optimization of selected L-tryptophan exporters, significantly improved precursor supply and export efficiency, leading to a substantial increase in L-tryptophan titer. Through iterative rounds of

model-guided engineering and metabolome analysis, a final strain capable of producing 16.2 g/L of L-tryptophan with a yield of 0.16 g/g glucose in shake-flask fermentations was achieved, demonstrating a yield comparable to reported *E. coli* producers. Notably, the engineered strain is plasmid-free and devoid of unknown mutations, representing a promising platform for industrial L-tryptophan production. Future efforts to further enhance L-tryptophan production can be directed towards the exploration of additional potential targets through multi-omics analyses and the optimization of fermentation processes.

Declaration of interests

None.

Acknowledgments

This work was supported by the National Key R&D Program of China (No. 2021YFC2100900), the National Natural Science Foundation of China (Grant Nos. 21938004, 22078172), and Tsinghua University Initiative Scientific Research Program (No. 20223080016).

Author Contributions

Yufei Dong: Methodology, Investigation, Formal analysis, Data curation, Validation, Writing-original draft preparation. Zhen Chen: Conceptualization, Investigation, Formal analysis, Writing - original draft, Writing - review & editing, Funding acquisition, Resources, Supervision, Project administration.

6 Reference

Baumgart, M., Unthan, S., Rückert, C., Sivalingam, J., Grünberger, A., Kalinowski, J., Bott, M., Noack, S., Frunzke, J., 2013. Construction of a prophage-free variant of *Corynebacterium glutamicum* ATCC 13032 for use as a platform strain for basic research and industrial biotechnology. Appl Environ Microbiol. 79, 6006-6015. https://doi.org/doi:10.1128/AEM.01634-13.

Caligiuri, M. G., Bauerle, R., 1991. Identification of amino acid residues involved in feedback regulation of the anthranilate synthase complex from *Salmonella typhimurium.* Evidence for an amino-terminal regulatory site. J Biol Chem. 266, 8328-8335. https://doi.org/10.1016/s0021-9258(18)92979-0.

Cao, M., Gao, M., Suástegui, M., Mei, Y., Shao, Z., 2020. Building microbial factories for the production of aromatic amino acid pathway derivatives: From commodity chemicals to

515 plant-sourced natural products. Metab Eng. 58, 94-132.
516 https://doi.org/10.1016/j.ymben.2019.08.008.
517 Chai, M., Deng, C., Chen, Q., Lu, W., Liu, Y., Li, J., Du, G., Lv, X., Liu, L., 2021. Synthetic biology
518 toolkits and metabolic engineering applied in *Corynebacterium glutamicum* for
519 biomanufacturing. ACS Synth Biol. 10, 3237-3250.
520 https://doi.org/10.1021/acssynbio.1c00355.
521 Chen, L., Zeng, A.-P., 2016. Rational design and metabolic analysis of *Escherichia coli* for effective
522 production of L-tryptophan at high concentration. Appl Microbiol Biotechnol. 101,
523 559-568. https://doi.org/10.1007/s00253-016-7772-5.
524 Chen, Z., Huang, J., Wu, Y., Wu, W., Zhang, Y., Liu, D., 2017. Metabolic engineering of
525 *Corynebacterium glutamicum* for the production of 3-hydroxypropionic acid from
526 glucose and xylose. Metab Eng. 39, 151-158.
527 https://doi.org/10.1016/j.ymben.2016.11.009.
528 Choi, K.-Y., 2020. A review of recent progress in the synthesis of bio-indigoids and their
529 biologically assisted end-use applications. Dyes Pigm. 181, 108570.
530 https://doi.org/10.1016/j.dyepig.2020.108570.
531 Cohen, S. A., Strydom, D. J., 1988. Amino acid analysis utilizing phenylisothiocyanate derivatives.
532 Anal Biochem. 174, 1-16.
533 https://doi.org/https://doi.org/10.1016/0003-2697(88)90512-X.
534 Dele-Osibanjo, T., Li, Q., Zhang, X., Guo, X., Feng, J., Liu, J., Sun, X., Wang, X., Zhou, W., Zheng, P.,
535 Sun, J., Ma, Y., 2019. Growth-coupled evolution of phosphoketolase to improve
536 l-glutamate production by *Corynebacterium glutamicum*. Appl Microbiol Biotechnol. 103,
537 8413-8425. https://doi.org/10.1007/s00253-019-10043-6.
538 Fang, X., Lloyd, C. J., Palsson, B. O., 2020. Reconstructing organisms in silico: genome-scale
539 models and their emerging applications. Nat Rev Microbiol. 18, 731-743.
540 https://doi.org/10.1038/s41579-020-00440-4.
541 Füller, J. J., Röpke, R., Krausze, J., Rennhack, K. E., Daniel, N. P., Blankenfeldt, W., Schulz, S., Jahn, D.,
542 Moser, J., 2016. Biosynthesis of violacein, structure and function of l-tryptophan oxidase
543 VioA from *Chromobacterium violaceum*. J Biol Chem. 291, 20068-20084.
544 https://doi.org/10.1074/jbc.M116.741561.
545 Guo, L., Ding, S., Liu, Y., Gao, C., Hu, G., Song, W., Liu, J., Chen, X., Liu, L., 2021. Enhancing
546 tryptophan production by balancing precursors in *Escherichia coli*. Biotechnol Bioeng.
547 119, 983-993. https://doi.org/10.1002/bit.28019.
548 Ikeda, M., 2006. Towards bacterial strains overproducing l-tryptophan and other aromatics by
549 metabolic engineering. Appl Microbiol Biotechnol. 69, 615-626.
550 https://doi.org/10.1007/s00253-005-0252-y.
551 Ikeda, M., Katsumata, R., 1999. Hyperproduction of tryptophan by *Corynebacterium glutamicum*
552 with the modified pentose phosphate pathway. Appl Environ Microbiol. 65, 2497–2502.
553 https://doi.org/10.1128/AEM.65.6.2497-2502.1999.
554 Ikeda, M., Katsumata, R., 2014. Tryptophan production by transport mutants of *Corynebacterium*
555 *glutamicum*. Biosci Biotechnol Biochem. 59, 1600-1602.
556 https://doi.org/10.1271/bbb.59.1600.
557 Ikeda, M., Nakanishi, K., Kino, K., Katsumata, R., 2014. Fermentative production of tryptophan by a
558 stable recombinant strain of *Corynebacterium glutamicum* with a modified

559 serine-biosynthetic pathway. Biosci Biotechnol Biochem. 58, 674-678.
560 https://doi.org/10.1271/bbb.58.674.
561 Jiang, Y., Sheng, Q., Wu, X.-Y., Ye, B.-C., Zhang, B., 2021. L-arginine production in
562 *Corynebacterium glutamicum*: manipulation and optimization of the metabolic process.
563 Crit Rev Biotechnol. 41, 172-185. https://doi.org/10.1080/07388551.2020.1844625.
564 Jun, K. H., Jang, J.-H., Rim, G. G., Lee, G. C., Huang, R., Pyo, H. H., 2015. CN 105143440 A. C. N. I. P.
565 Administration.
566 Kikuchi, Y., Tsujimoto, K., Kurahashi, O., 1997. Mutational analysis of the feedback sites of
567 phenylalanine-sensitive 3-deoxy-D-arabino-heptulosonate-7-phosphate synthase of
568 *Escherichia coli*. Appl Environ Microbiol. 63, 761-762.
569 https://doi.org/doi:10.1128/aem.63.2.761-762.1997.
570 Kogure, T., Inui, M., 2018. Recent advances in metabolic engineering of *Corynebacterium*
571 *glutamicum* for bioproduction of value-added aromatic chemicals and natural products.
572 Appl Microbiol Biotechnol. 102, 8685-8705.
573 https://doi.org/10.1007/s00253-018-9289-6.
574 Lee, J.-y., Lee, J.-h., 2020. Recent research progress in the microbial production of aromatic
575 compounds derived from L-tryptophan. J Life Sci. 30, 919-929.
576 https://doi.org/10.5352/JLS.2020.30.10.919
577 Li, Z., Dong, Y., Liu, Y., Cen, X., Liu, D., Chen, Z., 2022. Systems metabolic engineering of
578 *Corynebacterium glutamicum* for high-level production of 1,3-propanediol from
579 glucose and xylose. Metab Eng. 70, 79-88. https://doi.org/10.1016/j.ymben.2022.01.006.
580 Liu, J., Liu, M., Shi, T., Sun, G., Gao, N., Zhao, X., Guo, X., Ni, X., Yuan, Q., Feng, J., Liu, Z., Guo, Y.,
581 Chen, J., Wang, Y., Zheng, P., Sun, J., 2022a. CRISPR-assisted rational flux-tuning and
582 arrayed CRISPRi screening of an l-proline exporter for l-proline hyperproduction. Nat
583 Commun. 13, 891. https://doi.org/10.1038/s41467-022-28501-7.
584 Liu, J., Xu, J.-Z., Rao, Z.-M., Zhang, W.-G., 2022b. Industrial production of L-lysine in
585 *Corynebacterium glutamicum*: Progress and prospects. Microbiol Res. 262, 127101.
586 https://doi.org/10.1016/j.micres.2022.127101.
587 Liu, S., Wang, B.-B., Xu, J.-Z., Zhang, W.-G., 2023. Engineering of shikimate pathway and terminal
588 branch for efficient production of L-tryptophan in *Escherichia coli*. Int J Mol Sci. 24,
589 11866. https://doi.org/10.3390/ijms241411866.
590 Lv, Q., Hu, M., Tian, L., Liu, F., Wang, Q., Xu, M., Rao, Z., 2021. Enhancing l-glutamine production
591 in *Corynebacterium glutamicum* by rational metabolic engineering combined with a
592 two-stage pH control strategy. Bioresour Technol. 341, 125799.
593 https://doi.org/10.1016/j.biortech.2021.125799.
594 Mao, Z., Niu, J., Zhao, J., Huang, Y., Wu, K., Yun, L., Guan, J., Yuan, Q., Liao, X., Wang, Z., Ma, H.,
595 2024. ECMpy 2.0: A Python package for automated construction and analysis of
596 enzyme-constrained models. Synth Syst Biotechnol. 9, 494-502.
597 https://doi.org/10.1016/j.synbio.2024.04.005.
598 Mao, Z., Yuan, Q., Li, H., Zhang, Y., Huang, Y., Yang, C., Wang, R., Yang, Y., Wu, Y., Yang, S., Liao, X.,
599 Ma, H., 2023. CAVE: a cloud-based platform for analysis and visualization of metabolic
600 pathways. Nucleic Acids Res. 51, W70-W77. https://doi.org/10.1093/nar/gkad360 %J
601 Nucleic Acids Research.
602 Niu, H., Li, R., Liang, Q., Qi, Q., Li, Q., Gu, P., 2019. Metabolic engineering for improving

603 l-tryptophan production in *Escherichia coli*. J Ind Microbiol Biotechnol. 46, 55-65.
604 https://doi.org/10.1007/s10295-018-2106-5.
605 Niu, J., Mao, Z., Mao, Y., Wu, K., Shi, Z., Yuan, Q., Cai, J., Ma, H., 2022. Construction and analysis of
606 an enzyme-constrained metabolic model of *Corynebacterium glutamicum*. Biomolecules.
607 12. https://doi.org/10.3390/biom12101499.
608 O'Gara, J. P., Dunican, L. K., 1995. Mutations in the trpD gene of *Corynebacterium glutamicum*
609 confer 5-methyltryptophan resistance by encoding a feedback-resistant anthranilate
610 phosphoribosyltransferase. Appl Environ Microbiol. 61, 4477-4479.
611 https://doi.org/10.1128/aem.61.12.4477-4479.1995.
612 Peters-Wendisch, P., Netzer, R., Eggeling, L., Sahm, H., 2002. 3-Phosphoglycerate dehydrogenase
613 from *Corynebacterium glutamicum* : the C-terminal domain is not essential for activity
614 but is required for inhibition by L-serine. Appl Microbiol Biotechnol. 60, 437-441.
615 https://doi.org/10.1007/s00253-002-1161-y.
616 Sarwar, N., Sarwar, S., Ejaz, S., Al-Adeeb, A., Al-Ansi, W., Li, Y., Bai, Z., 2021. Metabolic engineering
617 of microorganisms to increase production of violacein. Int J Agric Environ Biotechnol. 6,
618 295-306. https://doi.org/10.22161/ijeab.61.37.
619 Shang, X., Zhang, Y., Zhang, G., Chai, X., Deng, A.-h., Liang, Y., Wen, T., 2013. Characterization
620 and molecular mechanism of AroP as an aromatic amino acid and histidine transporter in
621 *Corynebacterium glutamicum*. J Bacteriol. 195, 5334 - 5342.
622 https://doi.org/10.1128/JB.00971-13.
623 Shen, Y.-P., Niu, F.-X., Yan, Z.-B., Fong, L. S., Huang, Y.-B., Liu, J.-Z., 2020. Recent advances in
624 metabolically engineered microorganisms for the production of aromatic chemicals
625 derived from aromatic amino acids. Front Bioeng Biotechnol. 8, 407.
626 https://doi.org/10.3389/fbioe.2020.00407.
627 Tang, M., Pan, X., Yang, T., You, J., Zhu, R., Yang, T., Zhang, X., Xu, M., Rao, Z., 2023.
628 Multidimensional engineering of *Escherichia coli* for efficient synthesis of L-tryptophan.
629 Bioresour Technol. 386, 129475. https://doi.org/10.1016/j.biortech.2023.129475.
630 Tauch, A., Kirchner, O., Löffler, B., Götker, S., Pühler, A., Kalinowski, J., 2002. Efficient
631 electrotransformation of *Corynebacterium diphtheriae* with a mini-replicon derived from
632 the *Corynebacterium glutamicum* Plasmid pGA1. Curr Microbiol. 45, 362-367.
633 https://doi.org/10.1007/s00284-002-3728-3.
634 Unthan, S., Baumgart, M., Radek, A., Herbst, M., Siebert, D., Brühl, N., Bartsch, A., Bott, M.,
635 Wiechert, W., Marin, K., Hans, S., Krämer, R., Seibold, G., Frunzke, J., Kalinowski, J., Rückert,
636 C., Wendisch, V. F., Noack, S., 2014. Chassis organism from *Corynebacterium glutamicum*
637 – a top-down approach to identify and delete irrelevant gene clusters. Biotechnol J. 10,
638 290-301. https://doi.org/10.1002/biot.201400041.
639 Varma, A., Boesch, B. W., Palsson, B. O., 1993. Biochemical production capabilities of *Escherichia*
640 *coli*. Biotechnol Bioeng. 42, 59-73. https://doi.org/10.1002/bit.260420109.
641 Wang, J., Cheng, L.-K., Wang, J., Liu, Q., Shen, T., Chen, N., 2013. Genetic engineering of
642 *Escherichia coli* to enhance production of l-tryptophan. Appl Microbiol Biotechnol. 97,
643 7587-7596. https://doi.org/10.1007/s00253-013-5026-3.
644 Wang, J., Zhang, R., Zhang, J., Gong, X., Jiang, T., Sun, X., Shen, X., Wang, J., Yuan, Q., Yan, Y., 2021.
645 Tunable hybrid carbon metabolism coordination for the carbon-efficient biosynthesis of
646 1,3-butanediol in *Escherichia coli*. Green Chem. 23, 8694-8706.

https://doi.org/10.1039/d1gc02867g.

Wray, L. V., Fisher, S. H., 2010. Functional roles of the conserved Glu304 loop of *Bacillus subtilis* glutamine synthetase. J Bacteriol. 192, 5018-5025. https://doi.org/10.1128/jb.00509-10.

Wu, W., Zhang, Y., Liu, D., Chen, Z., 2019. Efficient mining of natural NADH-utilizing dehydrogenases enables systematic cofactor engineering of lysine synthesis pathway of *Corynebacterium glutamicum*. Metab Eng. 52, 77-86. https://doi.org/10.1016/j.ymben.2018.11.006.

Xiong, B., Zhu, Y., Tian, D., Jiang, S., Fan, X., Ma, Q., Wu, H., Xie, X., 2021. Flux redistribution of central carbon metabolism for efficient production of l-tryptophan in *Escherichia coli*. Biotechnol Bioeng. 118, 1393-1404. https://doi.org/10.1002/bit.27665.

Zha, J., Zhao, Z., Xiao, Z., Eng, T., Mukhopadhyay, A., Koffas, M. A. G., Tang, Y. J., 2023. Biosystem design of *Corynebacterium glutamicum* for bioproduction. Curr Opin Biotechnol. 79. https://doi.org/10.1016/j.copbio.2022.102870.

Zhang, J., Qian, F., Dong, F., Wang, Q., Yang, J., Jiang, Y., Yang, S., 2020. De novo engineering of *Corynebacterium glutamicum* for l-Proline production. ACS Synth Biol. 9, 1897-1906. https://doi.org/10.1021/acssynbio.0c00249.

Zhao, Z., Cai, M., Liu, Y., Hu, M., Yang, F., Zhu, R., Xu, M., Rao, Z., 2022. Genomics and transcriptomics-guided metabolic engineering *Corynebacterium glutamicum* for l-arginine production. Bioresour Technol. 364, 128054. https://doi.org/10.1016/j.biortech.2021.125799.